Behavior Characteristics of Cellulose Particles in Insulating Oil Gaps under a DC Electric Filed

Meng, Xuan ; Guo, Ruochen ; Wang, Haotian; Han, Xutao ; Zhang, Xuanrui ; Lin, Junhao

DOI
10.1109/TDEI.2024.3363112

Publication date
2024

Document Version
Final published version

Published in
IEEE Transactions on Dielectrics and Electrical Insulation

Behavior Characteristics of Cellulose Particles in Insulating Oil Gaps Under a DC Electric Filed

Xuan Meng, Ruochen Guo, *Member, IEEE*, Haotian Wang, Xutao Han, Xuanrui Zhang, and Junhao Li, *Senior Member, IEEE*

***Abstract*— During the long-term operation of converter transformers, the aging and decomposition of oil-paper insulation lead to the presence of cellulose particles in transformer oil, which affects the safe operation of the equipment. The motion characteristics of cellulose particles in short oil gaps and long oil gaps under a dc electric field are studied. The forces acting on a single particle, the aggregation characteristics of multiple particles, and the conditions for particle chain breakage are calculated and analyzed. An experimental platform is constructed to validate the conclusions. The results show that cellulose particles in transformer oil are subjected to the combined action of various forces under a dc electric field. Under the influence of the dipole force, multiple cellulose particles attract each other and form particle chains along the direction of the electric field. Changes in internal forces within the particle chain can cause the chain to break. The movement of particles in oil is closely related to the adsorption time of particle chains on the electrode surface and their movement time within the oil gap, which is affected by the resistivity, particle size, charge quantity, and external electric field intensity of the particles. In the experiments, particles form cellulose bridges in short oil gaps, while in long oil gaps, they move freely in transformer oil in the form of particle chains.**

***Index Terms*— Cellulose particle chains, contaminated transformer oil, converter transformer, dc voltage, long oil gap, particle motion, short oil gap.**

I. Introduction

TRANSFORMER oil plays an important role in the insulation and cooling of transformers, and the quality is crucial for the safe operation of power transformers [1], [2], [3]. With the long-term operation of converter transformers, the gradual aging and the decomposition of oil-paper insulation results in the presence of cellulose particles in transformer oil [4], [5], [6], [7]. The increase in cellulose particle content can lead to a decrease in the insulation strength of transformer oil, which is one of the important causes of transformer failures [8], [9], [10]. The movement and aggregation process of cellulose particles in transformer oil has always been a subject of great concern.

The impact of cellulose particles in converter transformers on the insulation performance of transformer oil is particularly evident [11], [12], [13]. The valve side of the converter transformer is subjected to an ac–dc composite voltage, and the dc component promotes the aggregation of cellulose particles [14], [15], [16]. The statistical report of CIGRE indicates that the valve side outlet of a converter transformer is the component with the highest electric field strength and failure rate [17]. The presence of solid particles, including cellulose particles, has a significant impact on this phenomenon. It also mentions that during the operation of the power grids, there are several transformer failures difficult to explain by factors other than particles. By improving the filtering devices or treating the transformer oil, the occurrence of such failures can be reduced. Additionally, in reports from many countries, many transformer failures were attributed to particles, and some failures occurred between high-voltage lead and turret, with the length of the oil gap reaching up to 400 mm. The insulation strength at the valve side outlet is more sensitive to particles, and the concentration distribution of the electric field and the presence of the long oil gap promote the aggregation of particles at the outlet. The flow rate of transformer oil in the valve side outlet is relatively slow, resulting in minimal influence on the movement characteristics of cellulose particles.

Previous studies have shown that cellulose particles have a significant impact on the dielectric strength of oil-paper insulation [18], [19], [20], [21]. Guo et al. [22], [23], [24] studied the effect of cellulose content levels in oil on the breakdown characteristics under lightning pulsed voltage, and an increase in the number of cellulose particles affects the insulation strength of transformer oil. Cellulose particles can form a cellulose bridge between the oil gap under high electric field. Zhao et al. [25] observed the moving process of cellulose particles in transformer oil under dc voltage, and found that the distortion of the electric field caused by the aggregation of cellulose particles promoted the growth of cellulose bridge. The type of voltage has a significant impact on the movement of particles in oil gaps. Liao et al. [26] applied dc, ac, and dc biased ac electric filed on the oil gap, respectively, during the experiments, and the results showed that the formation

Manuscript received 31 October 2023; revised 31 December 2023; accepted 3 February 2024. Date of publication 6 February 2024; date of current version 19 December 2024. This work was supported by the Shaanxi Science Foundation for Distinguished Young Scholars of China under Grant 2024JC-JCQN-42. *(Corresponding author: Junhao Li.)*

Xuan Meng, Haotian Wang, Xutao Han, Xuanrui Zhang, and Junhao Li are with the State Key Laboratory of Electrical Insulation and Power Equipment, Xi'an Jiaotong University, Xi'an 710049, China (e-mail: junhaoli@mail.xjtu.edu.cn).

Ruochen Guo is with the High Voltage Technologies Group, Faculty of Electrical Engineering, Mathematics and Computer Science, Delft University of Technology, 2628 CD Delft, The Netherlands.

Color versions of one or more figures in this article are available at https://doi.org/10.1109/TDEI.2024.3363112.

Digital Object Identifier 10.1109/TDEI.2024.3363112

of cellulose bridges was not observed only under ac electric field. Cellulose bridges formed by particles in transformer oil can affect the insulation strength. Li et al. [27] applied cellulose particles to transformer oil samples with different water contents and observed the leakage current under dc voltage. The presence of both cellulose and water caused the increase in leakage current, which leads to the water gasifying on the small bridge, generating a cellulose-gas bridge.

Previous researches on the movement of cellulose particles in transformer oil have primarily focused on the aspect of cellulose bridges in short oil gaps [28], [29]. However, the motion of cellulose particles in long oil gaps under dc electric field is different, and there is limited research on the characteristics of particle movement in such environments. Preliminary experimental results indicate that the formation of the cellulose bridge was not observed in the long oil gap. Cellulose particles aggregate to form particle chains, moving back and forth between the electrodes, accompanied by the aggregation and breakage of particle chains. Existing research has paid little attention to the interactions between multiple particles and have rarely analyzed the motion characteristics of particle chains, making it difficult to analyze the particle motion process in long oil gaps [30], [31], [32], [33]. Therefore, it is crucial to study the behavior characteristics of cellulose particles in short oil gaps and long oil gaps under a dc electric field.

This study mainly investigates the behavioral characteristics of cellulose particles in short oil gaps and long oil gaps under a dc electric field. The force on cellulose particles in transformer oil under the action of a dc electric field was statically analyzed from both external forces and interparticle forces. The aggregation process of multiple cellulose particles and the splitting process of cellulose particle chains were dynamically analyzed, summarizing the behavioral characteristics of particles in the oil gaps. Based on the variation of internal forces within particle chains, the factors influencing chain breakage under different conditions were analyzed through calculations. The differences in particle behavior characteristics between the short oil gap and long oil gap were observed experimentally.

II. Force Analysis

Cellulose particles are subjected to the combined action of multiple forces and move in transformer oil under the influence of the resultant force. The motion process of particles is unstable and the dynamics conditions are complex to analyze. Thus, a simplified treatment in the process of theoretical analysis is necessary. The behavior of particles in transformer oil can be divided into two parts, including the motion of individual particles in transformer oil and the interaction between multiple particles. The former is related to external field forces, while the latter is related to the interparticle forces. Based on the above two parts, a comprehensive analysis of forces acting on particles in transformer oil can be conducted.

A. External Forces

In transformer oil, individual particles are primarily influenced by several external forces, including dielectrophoretic (DEP) force, electric field force, and fluid drag force, in addition to gravity and buoyancy in the vertical direction. It is worth noting that cellulose is a nonmetallic material. In comparison with previous studies, the charging process is considered in this research

$$\boldsymbol{F}_{\mathrm{DEP}} = 2\pi {r_{\mathrm{p}}}^3 \varepsilon_{\mathrm{oil}} \left(\frac{\varepsilon_{\mathrm{P}} - \varepsilon_{\mathrm{oil}}}{\varepsilon_{\mathrm{P}} + 2\varepsilon_{\mathrm{oil}}} \right) \nabla \boldsymbol{E}^2 \tag{1}$$

$$\boldsymbol{F}_{\mathrm{C}} = kq\boldsymbol{E} \tag{2}$$

$$\boldsymbol{F}_{\mathrm{Drag}} = -6\pi \eta_{\mathrm{oil}} r_{\mathrm{p}} \boldsymbol{v} \tag{3}$$

$$\boldsymbol{F}_{\mathrm{G}} = \frac{4}{3}\pi r_{\mathrm{p}}^3 \rho_{\mathrm{p}} \boldsymbol{g} \tag{4}$$

$$\boldsymbol{F}_{\mathrm{B}} = \frac{4}{3}\pi r_{\mathrm{p}}^3 \rho_{\mathrm{oil}} \boldsymbol{g} \tag{5}$$

where r_{p} is the radius of cellulose particles. $\varepsilon_{\mathrm{oil}}$ and ε_{p} are the dielectric permittivity of transformer oil and cellulose particles, respectively. The parameter k is the correction factor, q is the amount of particle charge, and $\boldsymbol{E}$ is the external electric field strength at the location of particles. η_{oil} is the dynamic viscosity of transformer oil, and v is the velocity of particles in motion. ρ_{oil} and ρ_{p} are the density of transformer oil and cellulose particles, respectively.

According to (1), the DEP force experienced by cellulose particles is determined by the electric field strength and the relative dielectric constant of both transformer oil and cellulose particles. When the particle polarization rate exceeds that of the surrounding medium, an accumulation of charges occurs on the particle side at the solid–liquid interface. Under the influence of a nonuniform electric field, the polarized particles experience different forces at each end. The relative dielectric constant of transformer oil is 2.2, while that of cellulose is 4.2. Consequently, cellulose particles move toward regions of higher electric field strength, experiencing a positive DEP force.

Equation (2) is used to calculate the electric force on cellulose particles, where the parameter k is a correction factor that accounts for the influence of surface charges, and the calculation formula is as follows:

$$k = 0.832\left[1 + \frac{0.21(H-1)}{H-0.25}\right] \tag{6}$$

$$H = \frac{h}{r_{\mathrm{p}}} \tag{7}$$

where h is the distance between the particle center and the electrode, and r_{p} is the particle radius. The electric force on cellulose particles near the electrode is not constant but varies with the decreasing distance between the particles and the electrode. When the particles are close to the electrode surface, the value of k is 0.832, while it is 1 when they are far from the electrode.

The formula for calculating the charge on a spherical nonmetallic particle is as follows:

$$q_{\mathrm{s}} = \frac{2}{3}\pi^3 \varepsilon_{\mathrm{oil}} \varepsilon_0 \frac{\varepsilon_{\mathrm{p}}}{\varepsilon_{\mathrm{p}} + 2} r_{\mathrm{p}}^2 E \tag{8}$$

where q_{s} is the saturation charge on the nonmetallic particle. It is important to note that for nonmetallic particles, the charging process is not instantaneous, so the charge on the

particle can vary over time

$$q_0(t) = q_s\left(1 - e^{-\frac{t}{\tau_q}}\right) \tag{9}$$

$$\tau_q = \rho_c \varepsilon_p \varepsilon_0 \tag{10}$$

where τ_q is the relaxation time, and ρ_c is the resistivity of cellulose particles. When the resistivity of solid particles is high, the charge relaxation time is longer, resulting in a slower rate of change of the charge. Therefore, the charge on cellulose particles in transformer oil may not reach saturation, which should be analyzed in consideration of the actual situation.

According to (3), the drag force experienced by cellulose particles during their motion in oil is influenced by their velocity, radius, and the viscosity of the transformer oil. The direction of the drag force is opposite to the velocity of the particles, which inhibits an increase in their velocity.

B. Interparticle Forces

In previous studies, the influence of external forces on particles was often focused, but the interactions between multiple particles were rarely considered. While external forces are indeed capable of analyzing the motion of particles in oil, they hard to account for the aggregation behavior exhibited by particles within oil gaps. In this regard, interparticle forces, mainly including the Coulomb force and the dipole force, play an important role, and can be calculated as follows:

$$F_{Cij} = k_c \frac{q_i q_j}{{d_{ij}}^2} \tag{11}$$

$$\boldsymbol{F}_{\text{dipole}} = \sum_{j=1, j\neq i}^{n} (\boldsymbol{P_i} \cdot \nabla)\boldsymbol{E}_j \tag{12}$$

$$\boldsymbol{P}_i = 4\pi \varepsilon_{\text{oil}} \varepsilon_0 r_p^3 K \boldsymbol{E}_i \tag{13}$$

$$K = \frac{\varepsilon_p - \varepsilon_{\text{oil}}}{\varepsilon_p + 2\varepsilon_{\text{oil}}} \tag{14}$$

where k_c is the Coulomb's constant, q_i and q_j are the charges of the two particles, and d_{ij} is the distance between them. $\boldsymbol{P}_i$ is the electric dipole moment induced by the particle i under the influence of the external electric field $\boldsymbol{E}_i$, and $\boldsymbol{E}_j$ is the electric field strength induced by particle j at the location of particle i.

For a single cellulose particle with a radius of 50 μm in the electric field, the distribution of the normalized dipole force experienced by the surrounding free particles around it is shown in Fig. 1. The force distribution is symmetrical with the particle center. The regions near the particle along the direction parallel to the electric field, such as Region 1, tend to attract nearby free particles, while the regions perpendicular to the electric field direction, such as Region 2, tend to repel them.

For a free particle located at a distance d_{ij} from this particle, the dipole force experienced by the free particle at different positions, as well as the components of the dipole force along the direction of the electric field ($\boldsymbol{F}_\tau$) and perpendicular to the electric field direction ($\boldsymbol{F}_n$), have been calculated and shown in Fig. 2. Where θ is the angle between the line connecting particles and the direction perpendicular to the electric field. Based on the curves depicted in the figure, it can be observed

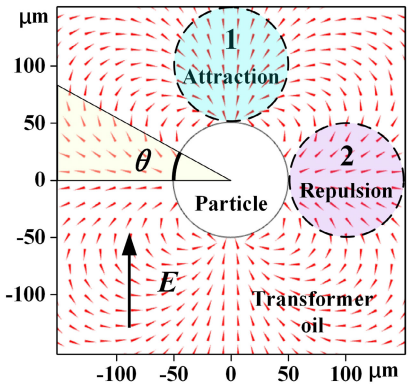

Fig. 1. Distribution of dipole force near a single particle.

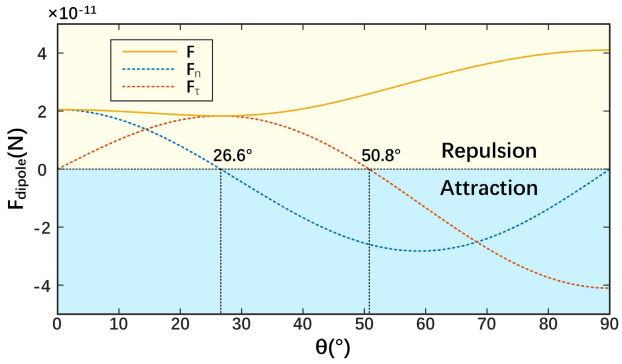

Fig. 2. Variation curves of the dipole force and the components at different positions.

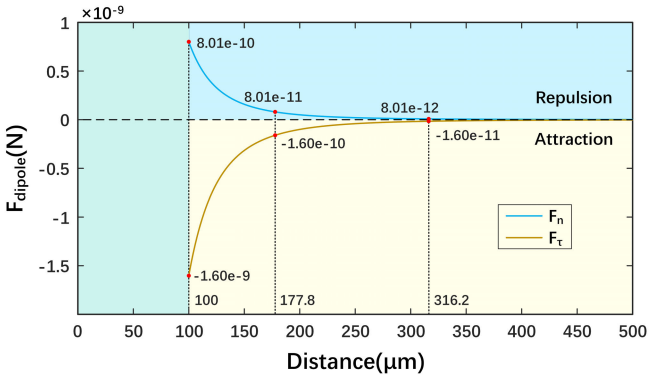

Fig. 3. Variation curves of dipole forces along the electric field direction and perpendicular to the electric field direction.

that the dipole force exhibits a repulsive effect when the angle theta is less than 26.6°, while it exhibits an attractive effect when the angle is greater than 50.8°.

Based on the source particle, by moving the free particle along the direction of the electric field and perpendicular to the electric field, the dipole force between the particles is calculated as shown in Fig. 3. The minimum distance is set to 100 μm, ensuring that the distance between the two particles remains greater than or equal to the sum of their radii.

The effect of the dipole force is the strongest when the particles are in direct contact with each other. However, once the particles separate, the effect rapidly weakens. The dipole

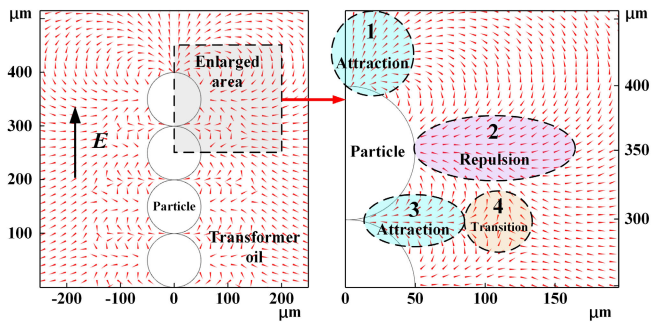

Fig. 4. Distribution of the dipole force near the end of the particle chain.

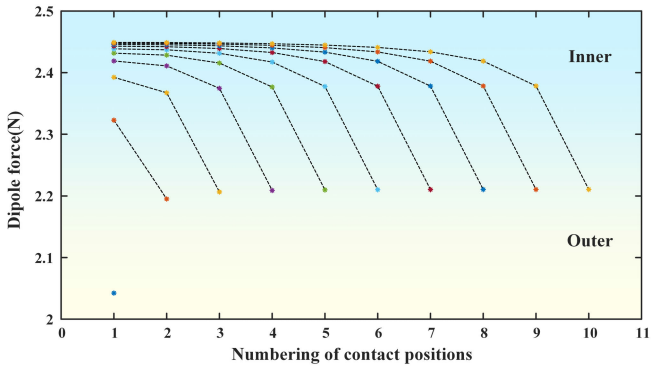

Fig. 5. Dipole forces at different positions within a particle chain.

force reaches its maximum value when the two particles are in contact. As the free particle moves away, the repulsive force perpendicular to the electric field direction rapidly decreases, reducing to 10% of the maximum value at a distance of 177.8 mm, decreasing to 1% of the maximum value at a distance of 316.2 mm, and then approaching zero. Similarly, the attractive force along the direction of the electric field also rapidly decreases as the free particle moves away. Therefore, the dipole force has a limited range of influence and decays quickly with increasing distance.

For cellulose particles in transformer oil, the charge quantity does not reach the saturation value. Compared to the dipole force, the effect of the Coulomb force between particles is relatively small. Therefore, the influence of the Coulomb force will not be taken into account in the subsequent discussion.

III. Motion of Multiple Particles

The changes in external forces and interparticle forces can have a significant impact on the motion characteristics of multiple particles, and these effects will be reflected in different oil gaps.

A. Aggregation of Multiple Particles

Driven by dipole forces, multiple cellulose particles mutually attract each other along the direction of the electric field, thereby forming a chain-like structure. A simulation model is constructed to calculate the dipole force around a particle chain under the dc electric field. Taking a particle chain composed of multiple particles as an example, the normalized dipole force experienced by a nearby free particle was calculated. The distribution of dipole force near the four particles at the end of the particle chain is shown in Fig. 4.

The four regions, highlighted by circles of different colors, exhibit the variations in the effect of the dipole force on the free particle. In regions 1 and 3, the free particles experience an attractive force, while in region 2, they experience a repulsive force. Region 4 is a transitional zone, where the free particles are subjected to a relatively weakened influence of dipole force. However, Region 3 is located in the middle of the particle chain, and the free particles experience repulsion from the dipole force before reaching this region, making it difficult for them to be adsorbed. On the other hand, the free particles are more likely to be adsorbed at region 1, which is the end of the particle chain. As free particles continuously adsorbed onto the end of the particle chain, the length of the cellulose particle chain increases.

In addition to the aggregation in the direction of the electric field, the dipole force also has a repulsive effect in the direction perpendicular to the electric field. For multiple different particle chains, the repulsive force affects the distance between the particle chains, limiting the packing density of the particle chain distribution. For the particle distribution inside a particle chain, the repulsive force affects the density of gaps between the particles and influences the volume distribution of the particle chain itself.

As the dipole force is independent of the position of the particle chain, the distribution of the dipole force near the particle chain on the electrode surface resembles that in Fig. 4. The side area of particle chains on the electrode surface exerts a repulsive effect on nearby free particles, making it difficult for them to move into this region. The top region of particle chains on the electrode surface, however, exerts an attractive force on the free particles. Therefore, when approaching the electrode surface, free particles are more easily adsorbed onto the top of the particle chains on the electrode surface.

Calculate the dipole forces at different positions within a particle chain composed of various numbers of particles, and the results are shown in Fig. 5.

The figure only displays a half-section of the particle chains, where the horizontal axis represents the numbering of contact positions between particles from the innermost to the outermost in the chains. The dipole force between the particles in a particle chain composed of two particles is only 2.04E-7 N. For longer particle chains, the maximum value of dipole force at the connection between particles occurs in the middle of the chain, while the outermost positions exhibit the minimum dipole force. For a particle chain composed of four particles, the maximum dipole force is only 2.32E-7 N. For a particle chain composed of ten particles, the maximum dipole force is only 2.43E-7 N. And for a particle chain composed of 20 particles, the maximum dipole force is only 2.45E-7 N. Due to the limited range of the dipole force, as the number of particles increases, the maximum dipole force within the particle chain approaches a constant value. Similarly, when the particle chain is composed of more than six particles, the minimum value of dipole force on the outermost positions of the particle chain also approaches a constant value.

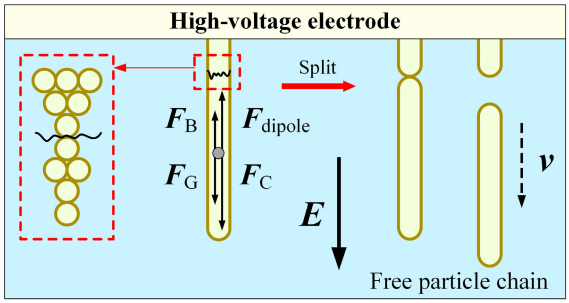

Fig. 6. Force analysis during the breaking process of particle chains.

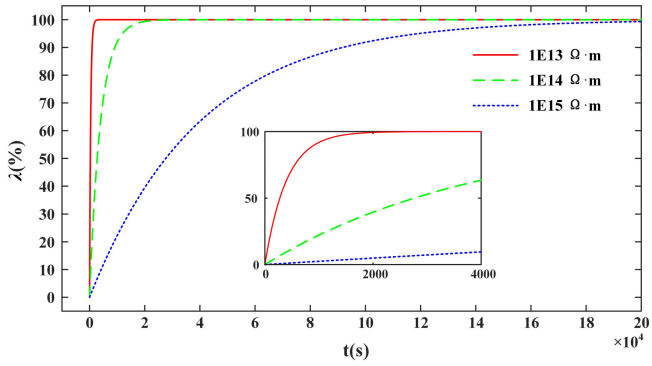

Fig. 7. Change of charge amount over time for cellulose particles with different resistivities.

B. Breakage of Particle Chains

The growth of particle chains caused by the attraction of the dipole force will not extend indefinitely. Under the influence of other forces, the breakage of particle chains can limit the increase in chain length. The forces acting on free particle chains in transformer oil exhibit minimal variations. However, particle chains on the surface of electrodes experience significant force changes due to varying charges. Theoretically, the breakage of particle chains typically occurs on the electrode surface. When a certain point of the cellulose particle chain reaches a force balance, the chain break at that point, as shown in Fig. 6.

For particle chains on the electrode surface, the amount of charge carried by each particle changes over time, which enhances the electric force in the direction away from the electrode under the external electric field. When the attractive dipole force can hardly balance the repulsive effect of other forces, the particle chain breaks.

The breaking positions in cellulose particle chains on electrode surfaces are closely related to forces on the particles. On the one hand, due to the limited range of the dipole force between particles, the maximum dipole force within particle chains approach a constant value. On the other hand, the effect of the external electric field force is closely related to the polarity and magnitude of the charges. The greater the number of particles on the outer side at a particular position within the particle chain, the greater the change in the total charge. Therefore, the variation in the external electric field force applied to it is also greater, making it easier to achieve force balance at the point. The longer the particle chain, the more prone it is to break. Theoretically, cellulose particle chains should break from the root. However, the distribution of particles within a particle chain itself is not uniform, and the dipole force at the connections between particles are also not constant. As a result, the location of particle chain breakage is uncertain in practice.

C. Behavioral Characteristics of Multiple Particles in Different Oil Gaps

According to the analysis of static particle forces and the dynamic behavior characteristics of particle chains, the process of particle motion in transformer oil is as follows.

1) Under the attractive effect of dipole forces, cellulose particles aggregate into particle chains of different lengths.
2) Particle chains can either float freely in transformer oil or attached to electrode surface, according to their location.
3) Under the influence of external forces, the freely floating particle chains move between the electrodes and connect to the surface particle chains at their tips.
4) Changes in the charge of the particles cause the breakage of particle chains on the electrode surface, forming new particle chains that float freely in transformer oil.

The aggregation state of particles in the oil gap is closely related to the distribution of particle chains between the electrodes. If the movement time of particle chains between the electrodes is longer, the particle chains tend to float freely in transformer oil. Correspondingly, if the charge variation rate of particle chains on the electrode surface is slow and the residence time of particle chains on the electrode surface is longer, the particle chains tend to stay on the electrode surface. Therefore, the characteristics of particle aggregation in the oil gap are closely related to the adsorption time of particle chains on the electrode surface and their movement time within the oil gap.

IV. Calculation

The adsorption time of particle chains on the electrode surface is microscopically manifested as the change rate of particle charge. The change of charge amount over time for cellulose particles with different resistivities is calculated, as shown in Fig. 7. The multiple of the particle charge amount relative to the saturation charge is denoted as λ.

In the initial stage, the particle charge changes rapidly, almost increasing linearly with time. As time goes on, the rate of change in particle charge gradually slows down. Eventually, the charge gradually approaches saturation. The rate of change in particle charge is closely related to its resistivity. When the resistivity is 1E13 Ω·m, it takes 42.0 s for λ to increase to 10%, and 917.4 s for it to increase to 90%. When the resistivity is 1E14 Ω·m, it takes 419.9 s for λ to increase to 10%, and 9174 s for it to increase to 90%. When the resistivity is 1E15 Ω·m, it takes 4198.6 s for λ to increase to 10%, and 91 740 s for it to increase to 90%. The higher the resistivity, the longer it takes for the particle charge to reach saturation.

The ease of particle chain breakage is closely related to the force effect, and it is necessary to analyze the conditions for

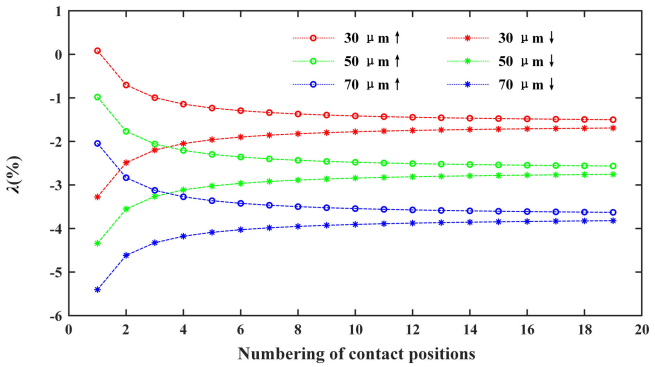

Fig. 8. Relationship between particle size and the value of λ when particle chains break.

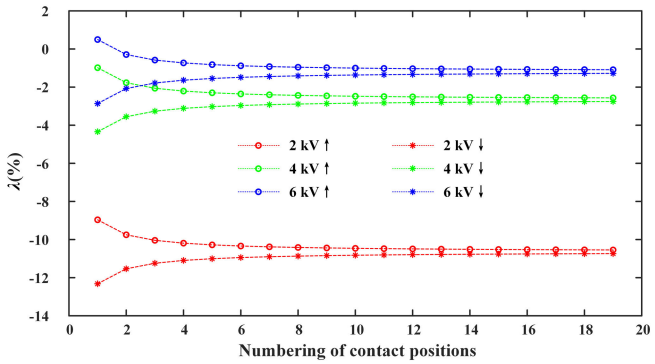

Fig. 9. Relationship between external electric field strength and the value of λ when particle chains break.

fracture at different positions within particle chains. Taking a particle chain adsorbed on the electrode surface in the vertical direction as an example, considering the dipole force between particles, the external electric field force acting on the particles, and the Gravity and Buoyancy, the particle charge when particle chains break under different conditions is calculated. The value of λ is calculated for different particle sizes under a constant vertical downward external electric field intensity of 4 kV/cm, as shown in Fig. 8. In the figure, the horizontal axis is the numbering of connection points between particles at the fracture location, which corresponds to the number of particles in the free particle chain formed after fracture. For particle chains of the same size, as the fracture position number increases, the value of λ decreases continuously for the particle chains adsorbed on the upper electrode surface, while it increases continuously for the particle chains adsorbed on the lower electrode surface. Eventually, the two curves stabilize near the same value.

This is because the increase in the number of particles has a smaller impact on the dipole forces between particles, while the external electric field force, gravity, and buoyancy have a more significant effect. Eventually, the force balance is reached between the external electric field force, gravity and buoyancy, leading to the stabilization of the particle charge when the particle chain breaks. For particle chains adsorbed on the lower electrode surface, the dipole force is directed downward, while the external electric field force provides an upward force. For particle chains adsorbed on the upper electrode surface, the dipole force is directed upward. However, if the dipole force is smaller than the gravity and buoyancy experienced by the particles, the external electric field force still provides an upward force. Here, the change in particle charge only alters its magnitude without changing its polarity. For the same number of particles, the value of λ decreases with an increase in particle size when the particle chain breaks. When there are ten particles outside the fracture position of the particle chain adsorbed on the surface of the upper electrode, the value of λ is -1.4% for particles with a radius of 30 μm, -2.5% for particles with a radius of 50 μm, and -3.5% for particles with a radius of 70 μm.

The value of λ is calculated for particles with a radius of 50 μm under different electric field strengths, as shown in Fig. 9.

For the same number of particles, the value of λ increases with an increase in electric field strength when the particle chain breaks. When there are ten particles outside the fracture position of the particle chain adsorbed on the surface of the upper electrode, the value of λ is -10.5% for an external electric field of 2 kV/cm, -2.5% for an external electric field of 3 kV/cm, and -1.0% for an external electric field of 4 kV/cm.

The region between the two curves is the range of particle charge changes. The smaller this range, the less charge change, and the less time it takes for a particle to change its charge. Therefore, the more particles in a particle chain, the easier it is to complete a charge change and thus break apart.

The movement time of particle chains in oil gaps depends on the velocity of the particle chains in transformer oil. The movement of the particle chains is primarily governed by the external electric field force, while the fluid drag force provides a restraining effect. The electric field force is related to the particle charge and the external electric field strength, while the fluid drag force increases with the increase in particle chain velocity, causing the movement velocity of the particle chain to quickly stabilize.

When the adsorption time of particle chains on the electrode surface is equal to their movement time within the oil gap, the length of the oil gap is considered as the critical length for forming cellulose bridges. In cases where the length of the oil gap is smaller than this critical value, particles in transformer oil tend to form cellulose bridges within the oil gap. However, when the length of the oil gap exceeds the critical value, particles in transformer oil are more likely to exist in the form of free particle chains in transformer oil.

V. Experimental Setup and Test Method

A. Insulation Model

The insulation models under dc high voltage were constructed to observe the movement of cellulose particles in short oil gap and long oil gap, respectively, as shown in Fig. 10.

The short oil gap model adopts a sphere-plane electrode configuration, where the sphere electrode is the high-voltage electrode with a diameter of 25 mm, and the plane electrode is the grounding electrode with a diameter of 100 mm. The distance between the sphere and the plane electrode is 10 mm.

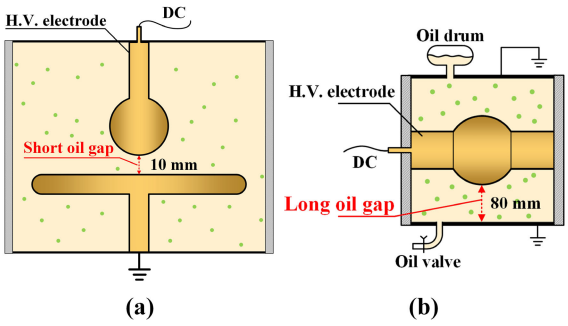

Fig. 10. Schematic of the insulation model. (a) Short oil gap insulation model and (b) long oil gap insulation model.

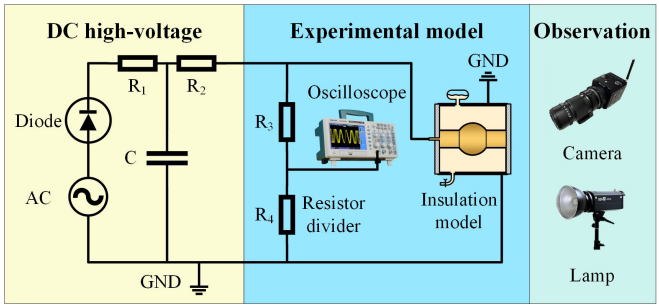

Fig. 11. Schematic of the test platform.

The uneven coefficient of the electric field distribution in the insulation model is 1.59, indicating a slightly nonuniform electric field.

The long oil gap model features a cubic structure with grounding plane electrodes at the top and bottom, and a high-voltage electrode in the center. The high-voltage electrode is cylindrical in shape with a spherical structure in the middle, allowing for observation of notable phenomena in the concentrated distribution area of the electric field. The diameter of the cylindrical part of the high-voltage electrode is 76 mm, and the diameter of the spherical part is 140 mm. The distance between the high-voltage electrode and the grounding electrode is 80 mm. The uneven coefficient of the electric field distribution in the insulation model is 1.75, indicating a slightly nonuniform electric field.

B. Oil Sample Pretreatment

Transformer oil with cellulose particles was added to the insulation model. The pretreatment of transformer oil can reduce the moisture and impurities in it, so as to obtain clean and dry transformer oil. The pretreatment process included transformer oil filtration and vacuum drying. The temperature of the vacuum drying oven was maintained at 80 °C, while the air pressure was kept below 133 Pa for a continuous period of 48 h. The cellulose particle size was controlled by sample sieves and subsequently subjected to a particle drying treatment. To prepare contaminated transformer oil samples, cellulose particles with a particle size ranging from 63 to 150 μm were incorporated into the transformer oil. And then, the transformer oil was stirred by using a magnetic stirrer for 5 min to achieve uniform distribution of cellulose particles.

C. Test Platform

The test platform, as shown in Fig. 11, consists of three components: a dc high voltage platform, an insulation model, and an observation platform. DC high voltage was added to the high-voltage electrode of the insulation model, and the movement of cellulose particles in oil was obtained based on the observation platform. In this study, a 4 kV dc voltage was applied to the short oil gap insulation model, resulting in an average electric field strength of 4 kV/cm and a maximum field strength of 6.37 kV/cm in the oil gap. Corresponding, a 32 kV dc voltage was applied to the long oil gap insulation model, resulting in an average electric field strength of 4 kV/cm and a maximum field strength of 6.9 kV/cm in the oil gap.

There were difficulties in observing the motion of particles in the long oil gap during the experiment. First, the long oil gap insulation model had a large volume, while the cellulose particles were small in size, making it challenging to observe the target particles. Second, due to the considerable distance between the equipment and the target particles, it was necessary to use a high-resolution camera capable of long duration recording to ensure clear observation of the particle motion in the insulation model. In addition, the lighting conditions in the experimental environment were complex and insufficient to generate clear images, which could affect the accuracy of the experimental results. In this study, a 6K resolution camera equipped with a macro lens of optical parameters (85 mm f/2.8) was utilized as the observation equipment, allowing for continuous recording of the localized particle motion within the long oil gaps. Additionally, a supplementary lamp was used to provide a uniform and bright lighting environment, and the lighting conditions were controlled during the experiment by adjusting the position, angle, and brightness of the supplementary lamp. In addition to the observation surface and the lighting surface, a black shading cloth was placed over the exterior of the insulation model to reduce the interference of ambient light. Experimental research was conducted based on the aforementioned insulation model.

VI. Experimental Result

By applying a dc high voltage to the high-voltage electrode, the motion process of particles in the two oil gaps was observed. The experimental results showed that there were significant differences in the motion characteristics of solid particles between long and short oil gaps, which were mainly reflected in the aggregation state and motion process of the particles.

A. Particles in the Short Oil Gap

Under the dc electric field, cellulose particles in the short oil gap formed cellulose bridges as the experiment progresses, as shown in Fig. 12.

At the initial moment, cellulose particles were uniformly floating in transformer oil. After applying a 4 kV dc voltage to the short oil gap model, cellulose particles in the oil began to move slowly between the electrodes. Cellulose particles had

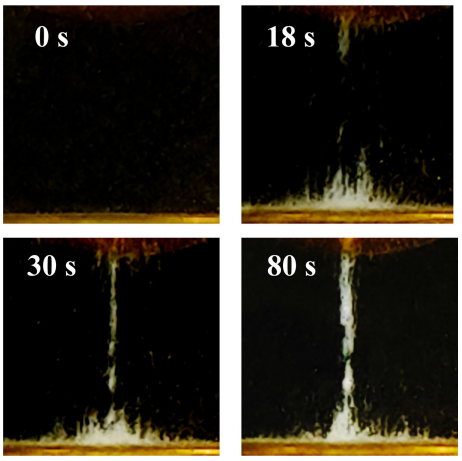

Fig. 12. Formation process of a cellulose bridge in the short oil gap.

already adhered to the surface of the electrode at 18 s. At 30 s, a complete cellulose bridge was formed for the first time. Subsequently, more and more cellulose particles accumulated between the electrodes, promoting the formation and growth of the bridge. At 80 s, the width of the cellulose bridge increased.

Before the formation of cellulose bridges, the movement of cellulose particles between the electrodes continued. In the short oil gap, the movement time of cellulose particles within the oil gap was about 0.1 s. However, the adsorption time of cellulose particles on the electrode surfaces was usually more than 0.5 s, which was much longer than the particle movement time within the oil gap.

B. Particles in the Long Oil Gap

Under the dc electric field, cellulose particles in the long oil gap aggregated into chains, floating freely in transformer oil or adsorbed on the electrode surface. The free particle chains exhibited straight chain-like structures, slightly pointed at the ends, with uneven particle distribution in the middle, as shown in Fig. 13(a). The particle chains attached to the electrode surface had a dense distribution, as shown in Fig. 13(b). The particles were densely distributed at the connection between the particle chain and the electrode, unevenly distributed in the middle of the chain, and exhibited a tip at the end. The particle chains were straight in shape and distributed perpendicular to the electrode surface.

The free particle chains moved back and forth in the oil gap. Particle chains attached to the electrode surface attracted and connected with the free particle chains, forming longer particle chains. The particle chains also broke on the electrode surface, resulting in new free particle chains moving in transformer oil. In the experiment, the majority of free particle chains had a length distribution below 4000 μm, while a small portion of longer particle chains reached lengths of up to 6000 μm.

In the long oil gap, cellulose particle chains moved back and forth between the high-voltage electrode and the grounding electrode. The normalized distribution of the electric field and the movement of cellulose particle chains between the electrodes in the long oil gap are shown in Fig. 14, with yellow arrows indicating the direction of the electric field.

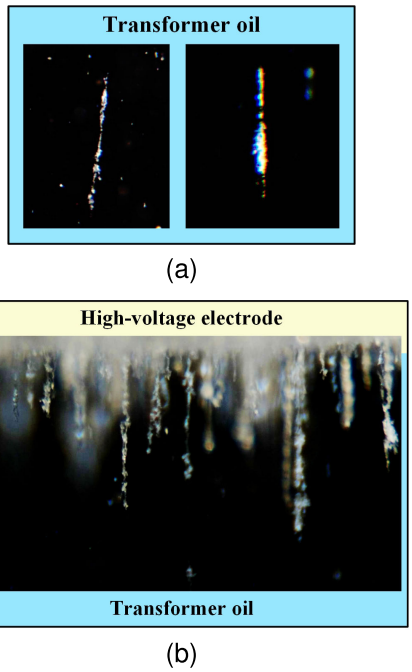

Fig. 13. Particle chains in the long oil gap. (a) Particle chains floating freely in transformer oil and (b) particle chains adsorbed on the electrode surface.

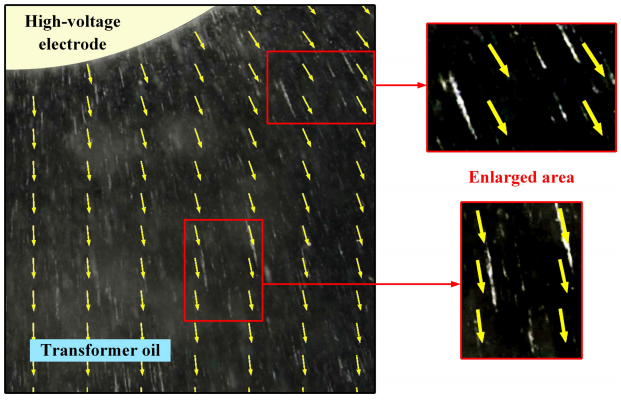

Fig. 14. Electric field distribution and movement of cellulose particle chains in the long oil gap.

By comparing them with the white cellulose particle chains, particularly in the enlarged areas, it can be observed that the direction of the free particle chains was consistent with the direction of the electric field at their respective locations.

Generally, the density of particle chains was higher in the lower portion of the model due to the influence of gravity, while the upper portion exhibited a rare distribution of free particle chains. Furthermore, the distribution of particle chains was concentrated below the high-voltage electrode, with fewer chains near the edges of the insulation model. The ascending velocity of particle chains below the high-voltage electrode was approximately 2.1 mm/s, while the descending velocity is around 2.5 mm/s. Particle chains near the edges of the model exhibit an ascending velocity of approximately 2.2 mm/s and a descending velocity of around 2.3 mm/s. Comparatively, the descending particle chains have relatively higher velocities than the ascending ones.

During the experiment, the particle chains adhered to the electrode surfaces often broke within 20 s. Therefore, the movement time c within the oil gap was much longer than the adsorption time of cellulose particles on the electrode surfaces.

In the long oil gap, the length of particle chains increased due to aggregation while being restricted by breakage. The free particle chains moved back and forth without forming microbridges between the electrodes, achieving a relative dynamic equilibrium.

By comparing the above results, it is evident that there are differences in the behavioral characteristic of particles in different oil gaps. In short oil gaps, particles had a shorter free time in transformer oil and were more likely to adsorb on the electrode surface, forming cellulose bridges between electrodes. On the other hand, in long oil gaps, particles had a shorter adsorption time on the electrode surface and spent most of the time freely moving in the transformer oil, reciprocating between electrodes in the form of particle chains.

VII. Conclusion

Based on the force and movement characteristics of cellulose particles in short oil gaps and long oil gaps under a dc electric field, the following conclusions can be drawn from theoretical analysis and experimental results.

Cellulose particles in transformer oil under a dc electric field are subjected to the combined action of multiple forces. External forces such as gravity, buoyancy, DEP force, electric field force, and fluid drag force mainly affect the motion of individual particles. Meanwhile, interparticle forces such as dipole force and Coulomb force mainly affect the interactions between multiple particles.

Under the influence of the dipole force, multiple cellulose particles are attracted to each other and form chain-like structures along the electric field direction. As the forces within the particle chains change, the chain will break at a point where an equilibrium of forces is reached. Multiple particles exhibit different behavioral characteristics in different oil gaps. The movement of particles in the oil is closely related to the adsorption time of particle chains on the electrode surface and the free movement time of particle chains within the oil gap.

The adsorption time of particle chains on the electrode surface is related to the resistivity, particle size, charge amount of cellulose particles and the external electric field strength. The free movement time of particle chains within the oil gap is related to the particle size and charge amount. When the adsorption time of particle chains on the electrode surface is equal to their movement time within the oil gap, the length of the oil gap is considered as the critical length for forming cellulose bridges.

A comparison was made between the particle movement characteristics in short oil gaps and long oil gaps under a dc electric field. In the short oil gap, complete cellulose bridges were formed between electrodes, and the adhesion time of particles on the electrode surface is much longer than their movement time within the oil gap. In long oil gaps, cellulose particles aggregate into chains, freely float in transformer oil or adhere to the electrode surface, and the movement time of particle chains within the oil gap is much longer than the adsorption time on the electrode surface. The length of particle chains increased due to aggregation while being restricted by breakage, achieving a relative dynamic balance in the movement of particles.

References

[1] Y. Zhang, J. Tang, C. Pan, and X. Luo, "Comparison of PD and breakdown characteristics induced by metal particles and bubbles in flowing transformer oil," *IEEE Access*, vol. 7, pp. 48098–48108, 2019, doi: 10.1109/ACCESS.2019.2910081.

[2] M. F. Rahman and P. Nirgude, "Partial discharge behaviour due to irregular-shaped copper particles in transformer oil with a different moisture content of pressboard barrier under uniform field," *IET Gener., Transmiss. Distribution*, vol. 13, no. 24, pp. 5550–5560, Dec. 2019, doi: 10.1049/iet-gtd.2019.0382.

[3] S. Mahmud, G. Chen, I. O. Golosnoy, G. Wilson, and P. Jarman, "Bridging phenomenon in contaminated transformer oil," in *Proc. IEEE Int. Conf. Condition Monitor. Diagnosis*, Sep. 2012, pp. 180–183, doi: 10.1109/CMD.2012.6416405.

[4] M. F. Rahman and P. Nirgude, "Irregular-shaped particle motion and charge transfer mechanism in transformer oil under varying field," in *Proc. IEEE 9th Power India Int. Conf. (PIICON)*, Sonepat, India, Feb. 2020, pp. 1–5.

[5] S. Mahmud, G. Chen, I. O. Golosnoy, G. Wilson, and P. Jarman, "Bridging in contaminated transformer oil under DC and AC electric field," *J. Phys. Conf. Ser.*, vol. 472, Nov. 2013, Art. no. 012007, doi: 10.1088/1742-6596/472/1/012007.

[6] M. H. S. Zainoddin, H. Zainuddin, and A. Aman, "Dielectrophoresis effect of dielectric liquids with suspended cellulose impurities under DC electric field," *Int. J. Electr. Comput. Eng. (IJECE)*, vol. 7, no. 6, p. 3254, Dec. 2017, doi: 10.11591/ijece.v7i6.pp3254-3261.

[7] Y. Li, K. Zhou, Z. R. Li, and Q. G. Zhang, "Research on the electrical aging characteristics of oil-impregnated pressboard under partial discharges," *IEEE Trans. Dielectr. Electr. Insul.*, vol. 27, no. 1, pp. 42–48, Feb. 2020, doi: 10.1109/TDEI.2019.008304.

[8] S. Saaidon, M. A. Talib, M. N. K. H. Rohani, N. A. Muhamad, and M. Kamarol, "The influences of cellulose bridging on the electrical field strength and thermal profile of PFAE under lightning impulse stress with DC superimposed," in *Proc. 9th Int. Conf. Condition Monitor. Diagnosis (CMD)*, Nov. 2022, pp. 172–176, doi: 10.23919/CMD54214.2022.9991697.

[9] J. Zhao, S. Zheng, H. Shao, C. Cheng, M. Fu, and R. Zhuo, "Breakdown in flowing transformer oil contaminated with cellulose particles under DC field," in *Proc. IEEE 6th Int. Electr. Energy Conf. (CIEEC)*, May 2023, pp. 1112–1116, doi: 10.1109/CIEEC58067.2023.10167340.

[10] N. A. M. Amin, M. T. Ishak, and N. S. Suhaimi, "Cellulose particles' effect on the electrical field distribution between palm oil and mineral oil insulation systems," in *Proc. IEEE Int. Conf. Power Energy (PECon)*, Dec. 2022, pp. 464–468, doi: 10.1109/PECon54459.2022.9988842.

[11] S. B. Saaidon, M. A. Talib, M. N. K. H. Rohani, N. A. Muhamad, and M. K. M. Jamil, "Breakdown voltage of transformer oil containing cellulose particle contamination with and without bridge formation under lightning impulse stress," *IEEE Access*, vol. 9, pp. 147994–148003, 2021, doi: 10.1109/ACCESS.2021.3124098.

[12] S. Xia et al., "Bridging characteristics of cellulosic particles in flowing transformer oil," *IEEE Trans. Dielectr. Electr. Insul.*, vol. 30, no. 3, pp. 1056–1065, Feb. 2023, doi: 10.1109/TDEI.2023.3241274.

[13] S. Xia, C. Pan, Y. Yao, Z. Wu, S. Mao, and J. Tang, "Accumulation characteristics of cellulose particles in flowing transformer oil under DC electric field," in *Proc. IEEE Int. Conf. High Voltage Eng. Appl. (ICHVE)*, Sep. 2022, pp. 1–4, doi: 10.1109/ICHVE53725.2022.10014510.

[14] M. H. S. Zainoddin, H. Zainuddin, and A. Aman, "Effects of viscosity of ester oils and different sizes of suspended cellulose particles on bridging phenomenon under non-uniform DC electric field," in *Proc. IEEE Int. Conf. Power Energy (PECon)*, Nov. 2016, pp. 285–289, doi: 10.1109/PECON.2016.7951574.

[15] L. Xining, T. Hao, Z. Shuqi, C. Huanchao, Y. Fan, and J. Shengchang, "The inner voltage component analysis and testing system for converter transformer valve side bushings," in *Proc. IEEE Int. Conf. High Voltage Eng. Appl. (ICHVE)*, Sep. 2020, pp. 1–4, doi: 10.1109/ICHVE49031.2020.9279817.

[16] S. Mahmud, G. Chen, I. O. Golosnoy, G. Wilson, and P. Jarman, "Experimental studies of influence of different electrodes on bridging in contaminated transformer oil," *IEEE Trans. Dielectr. Electr. Insul.*, vol. 22, no. 5, pp. 2433–2441, Oct. 2015, doi: 10.1109/Tdei.2015.004846.

[17] CIGRE, "Effect of particles on transformer dielectric strength," Work. Group 17 Study Committee 12, Paris, France, Tech. Rep. CIGRE 157, 2000, pp. 6–42. [Online]. Available: https://www.e-cigre.org/publications/detail/157-effect-of-particles-on-transformer-dielectric-strength.html

[18] W. Lu and Q. Liu, "Effect of cellulose particles on impulse breakdown in ester transformer liquids in uniform electric fields," *IEEE Trans. Dielectr. Electr. Insul.*, vol. 22, no. 5, pp. 2554–2564, Oct. 2015, doi: 10.1109/TDEI.2015.005097.

[19] T. Zhao, M. Fan, H. Yue, Y. Liu, and Z. Zhang, "Effect of cellulose particles on breakdown voltage in wet FR3 natural ester," *IEEE Access*, vol. 7, pp. 119357–119366, 2019.

[20] S. Mahmud, G. Chen, I. O. Golosnoy, G. Wilson, and P. Jarman, "Bridging in contaminated transformer oil under AC, DC and DC biased AC electric field," in *Proc. Annu. Rep. Conf. Electr. Insul. Dielectric Phenomena*, Oct. 2013, pp. 943–946, doi: 10.1109/CEIDP.2013.6747424.

[21] Y. Li et al., "Influence of fiber impurities on DC partial discharge process in oil-pressboard insulation," in *Proc. IEEE 19th Int. Conf. Dielectr. Liquids (ICDL)*, Jun. 2017, pp. 1–5, doi: 10.1109/ICDL.2017.8124660.

[22] R. Guo et al., "Breakdown characteristics of transformer oil with cellulose particles in a non-uniform field under lightning impulse voltage," *IEEE Trans. Dielectr. Electr. Insul.*, vol. 27, no. 5, pp. 1627–1635, Oct. 2020.

[23] R. Guo, Z. Wang, C. He, X. Meng, J. Li, and X. Han, "Impulse breakdown characteristics of transformer oil with cellulose particles in quasi-uniform field," *IEEE Trans. Dielectr. Electr. Insul.*, vol. 28, no. 1, pp. 107–115, Feb. 2021.

[24] R. Guo, Z. Sun, Z. Wang, C. He, X. Han, and J. Li, "Voltage-time characteristics of the different cellulose particle content transformer oil in a highly nonuniform field under lightning impulse," in *Proc. IEEE Int. Conf. High Voltage Eng. Appl. (ICHVE)*, Sep. 2020, pp. 1–4, doi: 10.1109/ICHVE49031.2020.9279424.

[25] T. Zhao, M. Fan, N. Chao, Y. Liu, and Z. Zhang, "The analysis of cellulose particles bridging in natural ester oil under DC voltage," in *Proc. IEEE 20th Int. Conf. Dielectr. Liquids (ICDL)*, Jun. 2019, pp. 1–4.

[26] R. Liao, M. Dan, J. Hao, L. Yang, and Y. Li, "Influence of oil aging on the motion characteristics of cellulose particles and conductivity in contaminated mineral oil and natural ester under DC electric field," *IEEJ Trans. Electr. Electron. Eng.*, vol. 13, no. 10, pp. 1384–1393, Oct. 2018, doi: 10.1002/tee.22776.

[27] Y. Li, K. Zhou, and H. Yuan, "Bridging and discharge mechanisms of cellulose impurities in transformer oil under DC voltage," *IEEE Trans. Dielectr. Electr. Insul.*, vol. 27, no. 3, pp. 1046–1049, Jun. 2020, doi: 10.1109/Tdei.2020.008658.

[28] J. Hao, R. Liao, M. Dan, Y. Li, J. Li, and Q. Liao, "Comparative study on the dynamic migration of cellulose particles and its effect on the conductivity in natural ester and mineral oil under DC electrical field," *IET Gener., Transmiss. Distrib.*, vol. 11, no. 9, pp. 2375–2383, Jun. 2017.

[29] Y. Li, K. Zhou, G. Y. Zhu, and Q. G. Zhang, "Effect of DC discharges in mineral oil on degradation characteristics of oil-impregnated pressboard," *IEEE Trans. Dielectr. Electr. Insul.*, vol. 26, no. 5, pp. 1701–1708, Oct. 2019, doi: 10.1109/TDEI.2019.008256.

[30] S. Mahmud, G. Chen, I. O. Golosnoy, G. Wilson, and P. Jarman, "Experimental studies of influence of DC and AC electric fields on bridging in contaminated transformer oil," *IEEE Trans. Dielectr. Electr. Insul.*, vol. 22, no. 1, pp. 152–160, Feb. 2015.

[31] X. Luo, C. Pan, Y. Yao, Y. Chen, and J. Tang, "Observation and simulation for the movement of metallic particles in flowing transformer oil under AC/DC and combined voltages," *IEEE Trans. Dielectr. Electr. Insul.*, vol. 28, no. 3, pp. 1034–1043, Jun. 2021, doi: 10.1109/TDEI.2021.009475.

[32] S. Mahmud, I. O. Golosnoy, G. Chen, G. Wilson, and P. Jarman, "Numerical simulation of charging and discharging of particles in contaminated transformer oil," in *Proc. IEEE Conf. Electr. Insul. Dielectric Phenomenon (CEIDP)*, Oct. 2017, pp. 588–591, doi: 10.1109/CEIDP.2017.8257502.

[33] S. Yang, Y. Li, K. Zhou, P. Duan, and H. Zhou, "Forming process of cellulose impurity bridge in oil-paper insulation under DC voltage," in *Proc. IEEE 4th Int. Conf. Electr. Mater. Power Equip. (ICEMPE)*, May 2023, pp. 1–4, doi: 10.1109/icempe57831.2023.10139610.

Xuan Meng was born in Henan, China, in 1995. He received the B.Sc. degree in electrical engineering from Xi'an Jiaotong University, Xi'an, Shaanxi, China, in 2019, where he is currently pursuing the Ph.D. degree in electrical engineering.

He is mainly engaged in fault detection and diagnosis technology of power equipment.

Ruochen Guo (Member, IEEE) was born in Shandong, China, in 1994. He received the Ph.D. degree in electrical engineering from Xi'an Jiaotong University, Xi'an, China.

From 2021 to 2022, he was a joint Ph.D. student at the KTH Royal Institute of Technology in the area of Applied Physics in Electrotechnology. Currently, he is a Researcher with the High Voltage Technology Group, Electrical Sustainable Energy Department, Delft University of Technology.

Haotian Wang was born in Xi'an, Shaanxi, China, in 1999. He received the B.Sc. degree in electrical engineering from Xi'an Jiaotong University, Xi'an, in 2020, where he is currently pursuing the Ph.D. degree.

Xutao Han received the Ph.D. degree in high voltage insulation technology from Xi'an Jiaotong University, Xi'an, China.

He is currently a Teacher with the State Key Laboratory of Electrical Insulation and Power Equipment, Xi'an Jiaotong University.

Xuanrui Zhang was born in Zhengzhou, Henan, China, in 1994. He received the Ph.D degree from Xi'an Jiaotong University, Xi'an, China, in 2023.

He is currently an Assistant Professor with Xi'an Jiaotong University. He focuses on the partial discharge detection and impulse test technology for power transformers.

Junhao Li (Senior Member, IEEE) was born in Xuchang, Henan, China, in 1980. He received the Ph.D. degree in electrical engineering from Xi'an Jiaotong University, Xi'an, China, in 2010.

He is currently a Professor with Xi'an Jiaotong University. He focuses on the detective and diagnostic techniques for electrical equipment.